ESAIM: M2AN 53 (2019) 1061–1082
https://doi.org/10.1051/m2an/2019012

ESAIM: Mathematical Modelling and Numerical Analysis
www.esaim-m2an.org

SUPERCONVERGENCE POINTS OF INTEGER AND FRACTIONAL DERIVATIVES OF SPECIAL HERMITE INTERPOLATIONS AND ITS APPLICATIONS IN SOLVING FDES

Beichuan Deng[1], Jiwei Zhang[2] and Zhimin Zhang[1,2,*]

Abstract. In this paper, we study the theory of convergence and superconvergence for integer and fractional derivatives of the one-point and two-point Hermite interpolations. When considering the integer-order derivatives, exponential decay of the error is proved, and superconvergence points are located, at which the convergence rates are $O(N^{-2})$ and $O(N^{-1.5})$ better than the global rates for the one-point and two-point interpolations, respectively. Here N represents the degree of the interpolation polynomial. It is proved that the αth fractional derivative of $(u-u_N)$, with $k<\alpha<k+1$, is bounded by its $(k+1)$-th derivative. Furthermore, the corresponding superconvergence points are predicted for fractional derivatives, and an eigenvalue method is proposed to calculate the superconvergence points for the Riemann–Liouville derivatives. In the application of the knowledge of superconvergence points to solve FDEs, we discover that a modified collocation method makes numerical solutions much more accurate than the traditional collocation method.

Mathematics Subject Classification. 65N35, 65M15, 26A33, 41A05, 41A10.

Received July 18, 2018. Accepted February 21, 2019.

1. Introduction

In recent years, Lagrange-type interpolation has been applied widely in numerical analysis, especially in the spectral Galerkin/collocation methods and numerical quadratures based on (weighted) orthogonal polynomials. Its usefulness stems from its stability and fast convergence for smooth functions. Recently, many works have focused on studying the superconvergence of Lagrange-type interpolations. For example, the superconvergence of integer-order derivatives of various Jacobi–Gauss-type spectral interpolations was considered in [27,28,33,34]. Zhang, Zhao and Deng generalized the study to Riemann–Liouville and Riesz fractional derivatives with the order of $0<\alpha<1$ in [7,35]. However, as pointed out in [7], Lagrange-type interpolations fail to converge when applied to the left Riemann–Liouville derivatives with $\alpha>1$. More specifically, the error ${}_{-1}D_x^{\alpha}(u-u_N)$ will not converge at $x=-1$, where u_N is the Legendre-Lobatto or Left-Radau interpolant of $u(x)$. The main reasonis

Keywords and phrases. Superconvergence, Hermite interpolation, Riemann–Liouville derivative, Riesz fractional derivative, generalized Jacobi polynomials, fractional differential equations.

[1] Department of Mathematics, Wayne State University, Detroit, MI 48202, USA.
[2] Beijing Computational Science Research Center, 100193 Beijing, PR China.
*Corresponding author: zmzhang@csrc.ac.cn

Article published by EDP Sciences

that the multiplicity of the root $x = -1$ of $u - u_N$ is one. Similarly, Lagrange-type interpolations also fail at $x = \pm 1$ when applied to Riesz fractional derivatives with $\alpha > 1$. This motivates us to find an alternative way to remedy the situations where Lagrange-type interpolations fail.

One candidate to remedy the failure of Lagrange-type interpolations is the Hermite interpolation. It is natural to consider this method because it can interpolate the function value at interior interpolation points, while also interpolating both the function value and the derivative value(s) at the two ends $x = \pm 1$. This results in a higher multiplicity of the roots at $x = \pm 1$. Consequently, Hermite interpolation resolves the difficulty posed by the singularities at the two ends, as compared with Lagrange-type interpolations. While the theory of convergence and superconvergence for Lagrange-type interpolations is well developed (see, [7, 27, 33–35]), the study on Hermite interpolation has, by comparison, received less attention and thus has more room for development.

The goal of this paper is to provide a fundamental analysis of the convergence and superconvergence for the integer-order and fractional derivatives of three kinds of Hermite interpolants; see definitions (3.1)–(3.3) below. It is proved that the integer-order derivative of the error of the Hermite interpolant, $(u - u_N)^{(k)}$, decays exponentially with respect to the degree of the interpolation polynomial N, when $u(x)$ is analytic on $[-1, 1]$. Moreover, for the one-point Hermite interpolation given by (3.1) or (3.2), the convergence rate at superconvergence points is $O(N^{-2})$ higher than the optimal global rate; for the two-point Hermite interpolation given by (3.3), it is $O(N^{-\frac{3}{2}})$ higher. Then, we apply the Hermite interpolations given in (3.1) and (3.2) to the left and right Riemann–Liouville derivatives, respectively, and (3.3) to the Riesz fractional derivative. A unified error estimate is given by

$$\|D^{\alpha}(u - u_N)\|_{\infty} \leqslant C\|(u - u_N)^{(k+1)}\|_{\infty},$$

where $k < \alpha < k + 1$, k is a nonnegative integer, and the constant C is independent of N. In other words, the convergence of the interpolation under the fractional derivatives is also guaranteed, and the error decays exponentially as well. In order to validate the superconvergence phenomenon under the Riemann–Liouville derivatives, an efficient algorithm to calculate superconvergence points is provided, and it is observed that the gain of convergence rate at these points is at least $O(N^{-1})$.

We emphasize that a systematic and rigorous mathematical treatment of superconvergence points of fractional derivatives can offer some theoretical insight into applications of numerically solving fractional differential equations (FDEs). It may also provide guidance when constructing numerical schemes that improve the numerical accuracy. Note that the fractional derivative of the Hermite interpolant $D^{\alpha}u_N$ approximates $D^{\alpha}u$ more accurately at the superconvergence points. This knowledge enables us to modify the traditional collocation method to solve FDEs: instead of using the traditional collocation points, the new collocation points are selected as the superconvegence points found in this paper. The existence and uniqueness of the numerical solution can be guaranteed based on the fact that the numbers of interpolation points and superconvergence points are equal to each other for fractional derivatives. Numerical experiments indicate that the accuracy of the modified collocation method results in an error at least 10^{-2} smaller than traditional collocation methods.

The paper is organized as follows. Preliminary knowledge is provided in Section 2. Sections 3–5 are about the theoretical statements of convergence and superconvergence of the Hermite interpolations for integer-order derivatives, the Riemann–Liouville derivative, and the Riesz derivative, respectively. Numerical validations and applications are presented in Section 6. Conclusions are drawn in Section 7.

2. Preliminaries

In this section, we begin with some basic definitions and properties, and denote $\mathbb{Z}^+$ and $\mathbb{N}$ by the sets of all positive integers and all nonnegative integers, respectively.

2.1. Definitions and properties of fractional derivatives

Let us first recall the definitions and properties of Riemann–Liouville and Riesz fractional derivatives.

Definition 2.1. For $\gamma \in (0,1)$, the left and right Riemann–Liouville integrals are defined respectively by

$$
\begin{aligned}
{}_{-1}I_x^{\gamma}u(x) &:= \frac{1}{\Gamma(\gamma)}\int_{-1}^{x}\frac{u(\tau)}{(x-\tau)^{1-\gamma}}\mathrm{d}\tau,\ x\in(-1,1],\\
{}_{x}I_1^{\gamma}u(x) &:= \frac{1}{\Gamma(\gamma)}\int_{x}^{1}\frac{u(\tau)}{(\tau-x)^{1-\gamma}}\mathrm{d}\tau,\quad x\in[-1,1).
\end{aligned}
$$

Then for $\alpha \in (k-1,k)$, where $k \in \mathbb{Z}^+$, the left and right Riemann–Liouville derivatives are defined respectively by:

$$
\begin{aligned}
{}_{-1}D_x^{\alpha}u(x) &= D^k({}_{-1}I_x^{k-\alpha}u(x))\\
&= \sum_{l=0}^{k-1}\frac{u^{(l)}(-1)}{\Gamma(l+1-\alpha)}(x+1)^{-\alpha+l} + {}_{-1}I_x^{k-\alpha}D^k u(x), \qquad (2.1)\\
{}_{x}D_1^{\alpha}u(x) &= (-1)^k D^k({}_{x}I_1^{k-\alpha}u(x))\\
&= \sum_{l=0}^{k-1}(-1)^l\frac{u^{(l)}(1)}{\Gamma(l+1-\alpha)}(1-x)^{-\alpha+l} + (-1)^k {}_{x}I_1^{k-\alpha}D^k u(x), \qquad (2.2)
\end{aligned}
$$

where $D^k := \frac{\mathrm{d}^k}{\mathrm{d}x^k}$ is the kth derivative.

Definition 2.2. Let $\gamma \in (0,1)$, the Riesz potentials in one dimension are defined as follows:

$$
I_o^{\gamma}u(x) := \frac{c_1}{\Gamma(\gamma)}\int_{-1}^{1}\frac{\mathrm{sign}(x-\tau)u(\tau)}{|x-\tau|^{1-\gamma}}\mathrm{d}\tau = c_1({}_{-1}I_x^{\gamma} - {}_{x}I_1^{\gamma})u(x), \qquad (2.3)
$$

$$
I_e^{\gamma}u(x) := \frac{c_2}{\Gamma(\gamma)}\int_{-1}^{1}\frac{u(\tau)}{|x-\tau|^{1-\gamma}}\mathrm{d}\tau = c_2({}_{-1}I_x^{\gamma} + {}_{x}I_1^{\gamma})u(x), \qquad (2.4)
$$

where $\mathrm{sign}(\cdot)$ represents the sign function, $c_1 = \frac{1}{2\sin(\pi\gamma/2)}$, $c_2 = \frac{1}{2\cos(\pi\gamma/2)}$. Then for $\alpha \in (k-1,k)$, we can therefore define the Riesz fractional derivative:

$$
{}^{R}D^{\alpha}u(x) := \begin{cases} D^k I_o^{k-\alpha}u(x) = c_1({}_{-1}D_x^{\alpha} + {}_{x}D_1^{\alpha})u(x),\ k \text{ is odd},\\ D^k I_e^{k-\alpha}u(x) = c_2({}_{-1}D_x^{\alpha} + {}_{x}D_1^{\alpha})u(x),\ k \text{ is even}. \end{cases} \qquad (2.5)
$$

2.2. Generalized Jacobi polynomials and their properties

We now address the definition of classical Jacobi polynomials and Generalized Jacobi Polynomials (GJP) with integer indexes. For the convenience of notations, the following four sets are introduced:

$$
\begin{aligned}
&\mathcal{Z}_1 = \{(\alpha,\beta)\in\mathbb{Z}^2 : \alpha,\beta < 0\}, && \mathcal{Z}_2 = \{(\alpha,\beta)\in\mathbb{Z}^2 : \alpha < 0, \beta \geqslant 0\},\\
&\mathcal{Z}_3 = \{(\alpha,\beta)\in\mathbb{Z}^2 : \alpha \geqslant 0, \beta < 0\}, && \mathcal{Z}_4 = \{(\alpha,\beta)\in\mathbb{Z}^2 : \alpha,\beta \geqslant 0\}.
\end{aligned}
$$

Definition 2.3. Let $\alpha,\beta > -1$. The classical Jacobi polynomials, denoted by $P_n^{\alpha,\beta}(x)$, are orthogonal with respect to the weight function $\omega^{\alpha,\beta}(x) = (1-x)^{\alpha}(1+x)^{\beta}$ over the interval $I = [-1,1]$, namely,

$$
\int_{-1}^{1} P_n^{\alpha,\beta}(x)P_m^{\alpha,\beta}(x)\omega^{\alpha,\beta}(x)\mathrm{d}x = \gamma_n^{\alpha,\beta}\delta_{m,n},
$$

where $\delta_{n,m}$ is the Kronecker function, and $\gamma_n^{\alpha,\beta} = \frac{2^{\alpha+\beta+1}\Gamma(n+\alpha+1)\Gamma(n+\beta+1)}{(n+\alpha+\beta+1)\Gamma(n+1)\Gamma(n+\alpha+\beta+1)}$.

Definition 2.4. Let $\alpha, \beta \in \mathbb{Z}$, the Generalized Jacobi Polynomial $\mathcal{J}_N^{\alpha,\beta}(x)$ is defined as follows:

$$\mathcal{J}_N^{\alpha,\beta}(x) = \begin{cases} (1-x)^{-\alpha}(1+x)^{-\beta}P_{\tilde{n}}^{-\alpha,-\beta}(x), & (\alpha,\beta) \in \mathcal{Z}_1, \tilde{n} = N+\alpha+\beta, \\ (1-x)^{-\alpha}P_{\tilde{n}}^{-\alpha,\beta}(x), & (\alpha,\beta) \in \mathcal{Z}_2, \tilde{n} = N+\alpha, \\ (1+x)^{-\beta}P_{\tilde{n}}^{\alpha,-\beta}(x), & (\alpha,\beta) \in \mathcal{Z}_3, \tilde{n} = N+\beta, \\ P_{\tilde{n}}^{\alpha,\beta}(x), & (\alpha,\beta) \in \mathcal{Z}_4, \tilde{n} = N, \end{cases} \tag{2.6}$$

where $\{\mathcal{J}_N^{\alpha,\beta}(x)\}$ are only defined for $N \geqslant -\min\{\alpha,0\} - \min\{\beta,0\}$, and $P_n^{\alpha,\beta}(x)$ is the classical Jacobi polynomial defined above.

It is easy to check that $\{\mathcal{J}_N^{\alpha,\beta}(x)\}$ is also a set of weighted orthogonal polynomials. This is, for any $\alpha, \beta \in \mathbb{Z}$, and $N, M \geqslant -\min\{\alpha,0\} - \min\{\beta,0\}$, we have:

$$\int_{-1}^{1} \mathcal{J}_N^{\alpha,\beta}(x)\mathcal{J}_M^{\alpha,\beta}(x)\omega^{\alpha,\beta}\mathrm{d}x = \eta_N^{\alpha,\beta}\delta_{N,M}, \tag{2.7}$$

where $\eta_N^{\alpha,\beta} = \gamma_{\tilde{n}}^{|\alpha|,|\beta|}$, and $\tilde{n}$ is defined in (2.6). Additionally, when both α, β are integers, according to [4,8,23], all of the GJPs satisfy the Sturm–Liouville equation:

$$\frac{\mathrm{d}}{\mathrm{d}x}[(1-x)^{\alpha+1}(1+x)^{\beta+1}\frac{\mathrm{d}}{\mathrm{d}x}\mathcal{J}_N^{\alpha,\beta}(x)] + \lambda_N^{\alpha,\beta}(1-x)^{\alpha}(1+x)^{\beta}\mathcal{J}_N^{\alpha,\beta}(x) = 0, \tag{2.8}$$

where $\lambda_N^{\alpha,\beta} = N(N+\alpha+\beta+1)$. It is well known that the classical Jacobi polynomials with $\alpha, \beta > -1$ satisfy

$$\frac{\mathrm{d}}{\mathrm{d}x}P_n^{\alpha,\beta}(x) = \frac{1}{2}(n+\alpha+\beta+1)P_{n-1}^{\alpha+1,\beta+1}(x), \ n \geqslant 1. \tag{2.9}$$

As for GJPs, we have similar formulas.

Lemma 2.5 (see [8], Lem. 2.1)**.** *If* $(\alpha,\beta) \in \mathcal{Z}_1$, *then*

$$\frac{\mathrm{d}}{\mathrm{d}x}\mathcal{J}_N^{\alpha,\beta}(x) = -2(N+\alpha+\beta+1)\mathcal{J}_{N-1}^{\alpha+1,\beta+1}(x); \tag{2.10}$$

if $(\alpha,\beta) \in \mathcal{Z}_2$, *then*

$$\frac{\mathrm{d}}{\mathrm{d}x}\mathcal{J}_N^{\alpha,\beta}(x) = -N\mathcal{J}_{N-1}^{\alpha+1,\beta+1}(x); \tag{2.11}$$

if $(\alpha,\beta) \in \mathcal{Z}_3$, *then*

$$\frac{\mathrm{d}}{\mathrm{d}x}\mathcal{J}_N^{\alpha,\beta}(x) = N\mathcal{J}_{N-1}^{\alpha+1,\beta+1}(x). \tag{2.12}$$

The following theorem states the maximum norm of GJPs.

Theorem 2.6. *Let* $\mathcal{J}_N^{\alpha,\beta}(x)$ *and* $\tilde{n}$ *be defined in (2.6), where* α, β *are integers. When* $\alpha = \beta < 0$, *if* $\tilde{n}$ *is even, then*

$$\|\mathcal{J}_N^{\alpha,\beta}(x)\|_{L^\infty[-1,1]} = |\mathcal{J}_N^{\alpha,\beta}(0)| = |P_{\tilde{n}}^{-\alpha,-\beta}(0)| = 2^{-\tilde{n}}\binom{\tilde{n}-\alpha}{\tilde{n}/2}, \tag{2.13}$$

if $\tilde{n}$ *is odd, then*

$$\|\mathcal{J}_N^{\alpha,\beta}(x)\|_{L^\infty[-1,1]} = |\mathcal{J}_N^{\alpha,\beta}(\eta_0)| \leqslant 2^{-\tilde{n}}\frac{\Gamma(\tilde{n}-\alpha+1)}{\Gamma(\tilde{n}/2+1)\Gamma(\tilde{n}/2-\alpha+1)}, \tag{2.14}$$

where η_0 is the zero point of $P_{\tilde{n}+1}^{-\alpha-1,-\alpha-1}(x)$ which is closest to 0; when $\alpha \leqslant 0$, $\beta \geqslant 0$, then

$$\|\mathcal{J}_N^{\alpha,\beta}(x)\|_{L^\infty[-1,1]} = |\mathcal{J}_N^{\alpha,\beta}(-1)| = 2^{|\alpha|}\binom{\tilde{n}+\beta}{\tilde{n}}; \tag{2.15}$$

when $\alpha \geqslant 0$, $\beta \leqslant 0$, then

$$\|\mathcal{J}_N^{\alpha,\beta}(x)\|_{L^\infty[-1,1]} = |\mathcal{J}_N^{\alpha,\beta}(1)| = 2^{|\beta|}\binom{\tilde{n}+\alpha}{\tilde{n}}, \tag{2.16}$$

where $\binom{n}{m} := \frac{n!}{m!(n-m)!}$ for integers n and m.

Proof. According to Lemma 2.5, the maximal value of $\mathcal{J}_N^{\alpha,\beta}(x)$ must be located at one of points in $A = \{-1, 1\} \cup \{\text{zeros of } P_{\tilde{n}+1}^{-\alpha-1,-\alpha-1}(x)\}$. Therefore, define

$$f(x) = \lambda_N^{\alpha,\beta}[\mathcal{J}_N^{\alpha,\beta}(x)]^2 + (1-x^2)\left[\frac{\mathrm{d}}{\mathrm{d}x}\mathcal{J}_N^{\alpha,\beta}(x)\right]^2, \ x \in [-1,1], \tag{2.17}$$

we can see that $\forall \eta \in A$,

$$f(\eta) = \lambda_N^{\alpha,\beta}[\mathcal{J}_N^{\alpha,\beta}(\eta)]^2,$$

so the question turns out to find

$$\max_{\eta\in A}\{f(\eta)\}.$$

By simplifying (2.8), we have:

$$(\alpha+\beta+2)x - \beta + \alpha = (1-x^2)\frac{\mathrm{d}^2}{\mathrm{d}x^2}\mathcal{J}_N^{\alpha,\beta}(x) + \lambda_N^{\alpha,\beta}\mathcal{J}_N^{\alpha,\beta}(x). \tag{2.18}$$

By inputting (2.18), we arrive at

$$\begin{aligned} f'(x) &= 2\frac{\mathrm{d}}{\mathrm{d}x}\left[\lambda_N^{\alpha,\beta}\mathcal{J}_N^{\alpha,\beta}(x) + (1-x^2)\frac{\mathrm{d}^2}{\mathrm{d}x^2}\mathcal{J}_N^{\alpha,\beta}(x) - x\cdot\frac{\mathrm{d}}{\mathrm{d}x}\mathcal{J}_N^{\alpha,\beta}(x)\right] \\ &= 2\left[\frac{\mathrm{d}}{\mathrm{d}x}\mathcal{J}_N^{\alpha,\beta}(x)\right]^2 \cdot [(\alpha+\beta+1)x - \beta + \alpha]. \end{aligned} \tag{2.19}$$

Hence $x^* = \frac{\beta-\alpha}{\alpha+\beta+1}$ is the only point that may change the sign of $f'(x)$. Then

(1) $|x^*| < 1 \ \Leftrightarrow \ (\alpha+\frac{1}{2})(\beta+\frac{1}{2}) > 0$,
(2) $|x^*| \geqslant 1 \ \Leftrightarrow \ (\alpha+\frac{1}{2})(\beta+\frac{1}{2}) \leqslant 0$.

Therefore, when $\alpha < 0$, $\beta \geqslant 0$, $f'(x) < 0$ on $[-1,1]$, we have

$$\|\mathcal{J}_N^{\alpha,\beta}(x)\|_{L^\infty[-1,1]} = |\mathcal{J}_N^{\alpha,\beta}(-1)| = 2^{|\alpha|}\binom{\tilde{n}+\beta}{\tilde{n}}.$$

When $\alpha \geqslant 0$, $\beta < 0$, $f'(x) > 0$ on $[-1,1]$, we have

$$\|\mathcal{J}_N^{\alpha,\beta}(x)\|_{L^\infty[-1,1]} = |\mathcal{J}_N^{\alpha,\beta}(1)| = 2^{|\beta|}\binom{\tilde{n}+\alpha}{\tilde{n}}.$$

When $\alpha = \beta < 0$, if $\tilde{n}$ is even, then $x^* = 0 \in A$ since $P_{\tilde{n}+1}^{-\alpha-1,-\alpha-1}(x)$ is an odd function, we have

$$\begin{aligned}\|\mathcal{J}_N^{\alpha,\beta}(x)\|_{L^\infty[-1,1]} = |\mathcal{J}_N^{\alpha,\beta}(0)| = |P_{\tilde{n}}^{-\alpha,-\beta}(0)| &= 2^{-\tilde{n}}\binom{\tilde{n}-\alpha}{\tilde{n}/2} \\ &= 2^{-\tilde{n}}\frac{\Gamma(\tilde{n}-\alpha+1)}{\Gamma(\tilde{n}/2+1)\Gamma(\tilde{n}/2-\alpha+1)},\end{aligned} \tag{2.20}$$

where (2.20) is derived from the three-recurrence formula of Jacobi polynomials. If $\tilde{n}$ is odd, since $x^* = 0 \notin A$, and $\mathcal{J}_N^{\alpha,\beta}(x)$ is an odd function, the absolute maximal value is obtained at $\pm\eta_0$, the zero point closest to 0, and we have:

$$\|\mathcal{J}_N^{\alpha,\beta}(x)\|_{L^\infty[-1,1]} = |\mathcal{J}_N^{\alpha,\beta}(\eta_0)| \leqslant 2^{-\tilde{n}}\frac{\Gamma(\tilde{n}-\alpha+1)}{\Gamma(\tilde{n}/2+1)\Gamma(\tilde{n}/2-\alpha+1)}.$$

The proof is complete. □

2.3. Interpolation of analytic functions

In this work, we always assume $u(x)$ is analytic on $[-1,1]$, and can be analytically extended to a certain domain on the complex-plane. The fundamental error analysis of Hermite interpolation was already provided in [5].

Lemma 2.7 (see [5], Thm. 3.5.1)**.** *Let $x_0, x_1, \ldots, x_n$ be $n+1$ distinct points in $[a,b]$. Let $m_0, m_1, \ldots, m_n$ be $n+1$ nonnegative integers. Let $N = (m_0 + \ldots + m_n) + n$. Designate by u_N the unique element of $\mathcal{P}_N$ for which*

$$u_N^{(k)}(x_i) = u^{(k)}(x_i), \quad k = 0, 1, \ldots, m_i, \quad i = 0, 1, \ldots, n, \tag{2.21}$$

where $u(x) \in C^N[a,b]$ and suppose that $u^{(N+1)}(x)$ exists in (a,b). Then

$$u(x) - u_N(x) := R_N(u;x) = \frac{u^{(N+1)}(\xi)}{(N+1)!}\omega_N(x), \tag{2.22}$$

where $\min(x, x_0, \ldots, x_m) < \xi < \max(x, x_0, \ldots, x_n)$, and

$$\omega_N(x) = (x - x_0)^{m_0+1}(x - x_1)^{m_1+1}\ldots(x - x_n)^{m_n+1}. \tag{2.23}$$

Lemma 2.8 (see [5], Cor. 3.6.3)**.** *Let $u(z)$ be analytic in a closed simply connected region R, $\mathcal{E}$ be a simple, closed, rectifiable curve that lies in R and contains the distinct points $x_0, x_1, \ldots, x_n$ in tis interior. Then*

$$u_N(x) = \frac{1}{2\pi i}\oint_{\mathcal{E}} \frac{\omega_N(z) - \omega_N(x)}{\omega_N(z)(z-x)}u(z)\mathrm{d}z \tag{2.24}$$

and

$$R_N(u;x) = \frac{1}{2\pi i}\oint_{\mathcal{E}} \frac{\omega_N(x)u(z)}{(z-x)\omega_N(z)}\mathrm{d}z, \tag{2.25}$$

where $u_N(x)$, $R_N(u;x)$, $\omega_N(x)$ are defined in (2.21), (2.22) and (2.23), respectively.

Without loss of generality, we usually consider functions that are analytic on the reference interval $[-1,1]$. It is known that each such function can be analytically extended to a domain enclosed by *Berstein ellipse* $\mathcal{E}_\rho$ with the foci ± 1, namely,

$$\mathcal{E}_\rho := \left\{ z : z = \frac{1}{2}(\rho e^{i\theta} + \rho^{-1}e^{-i\theta}),\ 0 \leqslant \theta < 2\pi,\ \rho > 1 \right\}, \tag{2.26}$$

where $i = \sqrt{-1}$ is the imaginary unit, ρ is the sum of semimajor and semiminor axes. Then we have the following bounds for $\mathcal{L}(\mathcal{E}_\rho)$, the perimeter of the ellipse, and $\mathcal{D}_\rho$, the shortest distance from $\mathcal{E}_\rho$ to $[-1, 1]$, respectively:

$$\mathcal{L}(\mathcal{E}_\rho) \leqslant \pi(\rho + \rho^{-1})^{\frac{1}{2}}, \text{ and } \mathcal{D}_\rho = \frac{1}{2}(\rho + \rho^{-1}) - 1. \tag{2.27}$$

For convenience, we define:

$$M_u^\rho = \sup_{z \in \mathcal{E}_\rho} |u(z)|. \tag{2.28}$$

3. Hermite interpolation for integer-order derivatives

In this work, we consider the three kinds of Hermite interpolations as follows.

(1) Let $-1 = x_0 < x_1 < \ldots < x_{\tilde{n}} < 1$ be $\tilde{n} + 1$ zeros of $\mathcal{J}_{N+1}^{0,-(k+1)}(x)$ (without considering multiplicity in all cases), where k is a positive integer, $\tilde{n} = N - k$. We are going to find $u_{NL}(x) \in \mathcal{P}_N([-1, 1])$, such that

$$\begin{aligned} u_{NL}^{(j)}(x_0) &= u^{(j)}(x_0),\ j = 0, \ldots, k, \text{ and} \\ u_{NL}(x_i) &= u(x_i),\ i = 1, \ldots, \tilde{n}. \end{aligned} \tag{3.1}$$

(2) Let $-1 < x_0 < x_1 < \ldots < x_{\tilde{n}} = 1$ be $\tilde{n} + 1$ zeros of $\mathcal{J}_{N+1}^{-(k+1),0}(x)$, where k is a positive integer, $\tilde{n} = N - k$. We are going to find $u_{NR}(x) \in \mathcal{P}_N([-1, 1])$, such that

$$\begin{aligned} u_{NR}^{(j)}(x_{\tilde{n}}) &= u^{(j)}(x_{\tilde{n}}),\ j = 0, \ldots, k, \text{ and} \\ u_{NR}(x_i) &= u(x_i),\ i = 0, \ldots, \tilde{n} - 1. \end{aligned} \tag{3.2}$$

(3) Let $-1 = x_0 < x_1 < \ldots < x_{\tilde{n}+1} = 1$ be $\tilde{n} + 2$ zeros of $\mathcal{J}_{N+1}^{-(k+1),-(k+1)}(x)$, where k is a positive integer, $\tilde{n} = N - 2k - 1$. We are going to find $u_{NB}(x) \in \mathcal{P}_N([-1, 1])$, such that

$$\begin{aligned} &u_{NB}^{(j)}(x_s) = u^{(j)}(x_s),\ j = 0, 1, \ldots, k,\ s = 0, \tilde{n} + 1, \text{ and} \\ &u_{NB}(x_i) = u(x_i),\ i = 1, 2, \ldots, \tilde{n}. \end{aligned} \tag{3.3}$$

Clearly, if (3.1) is applied, then $x = -1$ will be a zero point of $(u - u_N)$ of multiplicity $k + 1$; if (3.2) is applied, then $x = 1$ will be a zero point of multiplicity $k + 1$; if (3.3) is applied, then both $x = \pm 1$ are zero points of multiplicity $k + 1$.

Let us first discuss the interpolation errors. According to (2.22) and Theorem 2.6, we immediately derive the following corollary.

Corollary 3.1. *Let u_{NL} and u_{NR} be the interpolants defined in (3.1) and (3.2), respectively, and $-(\min\{\alpha, 0\} + \min\{\beta, 0\}) \leqslant N$. Then*

$$|R_N(u; x)| \leqslant \frac{2^{N+1}\Gamma(N - k + 1)}{\Gamma(2N - k + 2)} \|u^{(N+1)}(x)\|_{C[-1,1]}. \tag{3.4}$$

Let u_{NB} be the interpolant defined in (3.3). Then

$$|R_N(u; x)| \leqslant \frac{\Gamma(N - 2k)\Gamma(N - k + 1)\|u^{(N+1)}(x)\|_{C[-1,1]}}{\Gamma(2N - 2k + 1)\Gamma((N + 1)/2 - k)\Gamma((N + 1)/2 + 1)}. \tag{3.5}$$

Besides Corollary 3.1, another error representation is given by (2.25). We now focus on finding the superconvergence points $\{\xi_i\}$ in the sense of

$$N^{\beta} \max_{-1\leqslant\xi_i\leqslant 1} |(u-u_N)^{(k+1)}(\xi_i)| \lesssim \max_{-1\leqslant x\leqslant 1} |(u-u_N)^{(k+1)}(x)|, \tag{3.6}$$

where u_N is one of u_{NL}, u_{NR}, u_{NB}, k is the number given by (3.1), (3.2) and (3.3), respectively, and β is the gain of convergence rate. The superconvergence points $\{\xi_i\}$ and β are determined by the type of interpolants. Following the analysis in [34], we can obtain the following theorem.

Theorem 3.2. *Let $u(x)$ be analytic on $[-1,1]$ and within Berstein Ellipse $\mathcal{E}_\rho$ defined in (2.26) with $\rho>1$, and let u_{NL}, u_{NR}, u_{NB} be the interpolants defined in (3.1), (3.2) and (3.3), respectively. Suppose $k\ll N$, then we obtain the global error estimates as follows. For the interpolant u_{NL}, we have*

$$\max_{-1\leqslant x\leqslant 1} |(u-u_{NL})^{(k+1)}(x)| \leqslant c_1 M_u^{\rho} \left(1+\frac{D_\rho}{2}N^2\right)^{k+1} \frac{\tilde{n}^{\frac{1}{2}}}{\rho^{\tilde{n}}}, \tag{3.7}$$

the superconvergence points $\{\xi_L^i\}_{i=1}^{N-k}$ are zero points of $P_{N-k}^{k+1,0}(x)$, and

$$\max_{1\leqslant i\leqslant N-k} |(u-u_{NL})^{(k+1)}(\xi_L^i)| \leqslant c_1' M_u^{\rho} \left(1+\frac{D_\rho}{2}N^2\right)^{k} \frac{\tilde{n}^{\frac{1}{2}}}{\rho^{\tilde{n}}}. \tag{3.8}$$

For the interpolant u_{NR}, we have

$$\max_{-1\leqslant x\leqslant 1} |(u-u_{NR})^{(k+1)}(x)| \leqslant c_1 M_u^{\rho} \left(1+\frac{D_\rho}{2}N^2\right)^{k+1} \frac{\tilde{n}^{\frac{1}{2}}}{\rho^{\tilde{n}}}, \tag{3.9}$$

the superconvergence points $\{\xi_R^i\}_{i=1}^{N-k}$ are zero points of $P_{N-k}^{0,k+1}(x)$, and

$$\max_{1\leqslant i\leqslant N-k} |(u-u_{NR})^{(k+1)}(\xi_R^i)| \leqslant c_1' M_u^{\rho} \left(1+\frac{D_\rho}{2}N^2\right)^{k} \frac{\tilde{n}^{\frac{1}{2}}}{\rho^{\tilde{n}}}. \tag{3.10}$$

For the interpolant u_{NB}, we have

$$\max_{-1\leqslant x\leqslant 1} |(u-u_{NB})^{(k+1)}(x)| \leqslant c_2 M_u^{\rho} (N^{k+1}+O(N^{k-\frac{1}{2}})) \frac{\tilde{n}^{\frac{1}{2}}}{\rho^{\tilde{n}}}, \tag{3.11}$$

the superconvergence points $\{\xi_B^i\}_{i=1}^{N-k}$ are zero points of $P_{N-k}^{0,0}(x)$, and

$$\max_{1\leqslant i\leqslant N-k} |(u-u_{NB})^{(k+1)}(\xi_B^i)| \leqslant c_2' M_u^{\rho} \left(1+\frac{2}{e}N\right)^{k} N^{-\frac{1}{2}} \frac{\tilde{n}^{\frac{1}{2}}}{\rho^{\tilde{n}}}, \tag{3.12}$$

where c_i, c_i', $i=1,2$, only depend on ρ, k.

Proof. Since u_{NL} and u_{NR} are completely symmetric, without loss of generality, we only consider the cases of u_{NL} and u_{NB} in the proof. According to (2.25), we have

$$\begin{aligned} D^{k+1}(u(x)-u_N(x)) &= D^k R_N(u;x) \qquad (3.13)\\ &= \frac{1}{2\pi i}\oint_{\mathcal{E}_\rho} D^{k+1}\left(\frac{\omega_{N+1}(x)}{z-x}\right)\frac{u(z)}{\omega_{N+1}(z)}\mathrm{d}z \\ &= \frac{1}{2\pi i}\sum_{l=0}^{k+1}\binom{k+1}{l}\oint_{\mathcal{E}_\rho}\frac{D^l\omega_{N+1}(x)}{(z-x)^{k-l+2}}\frac{u(z)}{\omega_{N+1}(z)}\mathrm{d}z, \qquad \forall x\in[-1,1]. \qquad (3.14) \end{aligned}$$

If $u_N(x) = u_{NL}(x)$, then $\omega_{N+1}(x) = (A_{\tilde{n}}^{0,k+1})^{-1}\mathcal{J}_{N+1}^{0,-(k+1)}(x)$, where $A_{\tilde{n}}^{0,k+1}$ denotes the leading coefficient. Since there is a $\omega_{N+1}(z)$ in the denominator, we just consider $\omega_{N+1}(x) = \mathcal{J}_{N+1}^{0,-(k+1)}(x)$. According to Lemma 2.5, we have

$$D^l\omega_{N+1}(x) = \frac{\Gamma(N+2)}{\Gamma(N-l+2)}\mathcal{J}_{N+1-l}^{l,-k-1+l}(x),\ l = 0, 1, \ldots, k+1. \tag{3.15}$$

When N is large enough ($N \geqslant 3$), we arrive at

$$\max_{-1\leqslant x\leqslant 1}|D^l\omega_{N+1}(x)| = \frac{\Gamma(N+2)}{\Gamma(N-l+2)}2^{k+1-l}\binom{\tilde{n}+l}{\tilde{n}} \leqslant 2^{k+2}(\frac{N^2}{2})^l, \tag{3.16}$$

where $\tilde{n} = N-k$. On the other hand, according to the analysis in ([27], (4.7)), $\forall \rho > 1, k \in \mathbb{N}$, $\exists C_1(\rho,k) > 0$, such that

$$\min_{z\in\mathcal{E}_\rho}|P_{\tilde{n}}^{0,k+1}(z)| \geqslant C_1(\rho,k)\tilde{n}^{-\frac{1}{2}}\rho^{\tilde{n}}. \tag{3.17}$$

Noting that

$$\min_{z\in\mathcal{E}_\rho}|(1+z)^{k+1}| = D_\rho^{k+1},$$

and from (2.6), we have

$$\begin{aligned}\min_{z\in\mathcal{E}_\rho}|\mathcal{J}_{N+1}^{0,-(k+1)}(z)| &\geqslant \min_{z\in\mathcal{E}_\rho}|(1+z)^{k+1}| \cdot \min_{z\in\mathcal{E}_\rho}|P_{\tilde{n}}^{0,k+1}(z)| \\ &\geqslant C_1(\rho,k)D_\rho^{k+1}\tilde{n}^{-\frac{1}{2}}\rho^{\tilde{n}}.\end{aligned} \tag{3.18}$$

The identity (3.14) thus turns out to be

$$\frac{1}{2\pi i}\sum_{l=0}^{k+1}\binom{k+1}{l}\frac{\Gamma(N+2)}{\Gamma(N-l+2)}\oint_{\mathcal{E}_\rho}\frac{\mathcal{J}_{N+1-l}^{l,-k-1+l}(x)}{(z-x)^{k+2-l}}\frac{u(z)}{\mathcal{J}_{N+1}^{0,-(k+1)}(z)}\mathrm{d}z \tag{3.19}$$

$$\begin{aligned}&\leqslant \frac{1}{2\pi}\sum_{l=0}^{k+1}\binom{k+1}{l}\frac{\Gamma(N+2)}{\Gamma(N-l+2)}\oint_{\mathcal{E}_\rho}\frac{|\mathcal{J}_{N+1-l}^{l,-k-1+l}(x)|}{|(z-x)|^{k+2-l}}\frac{|u(z)|}{|\mathcal{J}_{N+1}^{0,-(k+1)}(z)|}\mathrm{d}|z| \\ &\leqslant \frac{1}{2\pi}\sum_{l=0}^{k+1}\binom{k+1}{l}2^{k+2}(\frac{N^2}{2})^l\frac{M_u^\rho\mathcal{L}(\mathcal{E}_\rho)}{D_\rho^{k+2-l}}\cdot\frac{\tilde{n}^{\frac{1}{2}}}{C_1(\rho,k)D_\rho^{k+1}\rho^{\tilde{n}}} \\ &= M_u^\rho\frac{2^{k+1}\mathcal{L}(\mathcal{E}_\rho)}{\pi C_1(\rho,k)D_\rho^{2k+3}}\frac{\tilde{n}^{\frac{1}{2}}}{\rho^{\tilde{n}}}\sum_{l=0}^{k+1}\binom{k+1}{l}\left(\frac{D_\rho}{2}N^2\right)^l \\ &= M_u^\rho\frac{2^{k+1}\mathcal{L}(\mathcal{E}_\rho)}{\pi C_1(\rho,k)D_\rho^{2k+3}}\frac{\tilde{n}^{\frac{1}{2}}}{\rho^{\tilde{n}}}\left(1+\frac{D_\rho}{2}N^2\right)^{k+1}.\end{aligned} \tag{3.20}$$

When $x = \xi_L^i$, $i = 1, \ldots, N-k$, where $\{\xi_L^i\}_{i=1}^{N-k}$ are zero points of $P_{N-k}^{k+1,0}(x)$, the last term in (3.19) vanishes. This is, for $1 \leqslant i \leqslant N-k$, we have

$$\begin{aligned}&|D^{k+1}(u(\xi_L^i) - u_N(\xi_L^i))| \\ &\quad= \frac{1}{2\pi i}\sum_{l=0}^{k}\binom{k+1}{l}\frac{\Gamma(N+2)}{\Gamma(N-l+2)}\left|\oint_{\mathcal{E}_\rho}\frac{\mathcal{J}_{N+1-l}^{l,-k-1+l}(\xi_L^i)}{(z-\xi_L^i)^{k+2-l}}\frac{u(z)}{\mathcal{J}_{N+1}^{0,-(k+1)}(z)}\mathrm{d}z\right|\end{aligned}$$

$$\leqslant M_u^\rho \frac{2^{k+1}\mathcal{L}(\mathcal{E}_\rho)}{\pi C_1(\rho,k)D_\rho^{2k+3}} \frac{\tilde{n}^{\frac{1}{2}}}{\rho^{\tilde{n}}} \sum_{l=0}^{k} \binom{k+1}{l} \left(\frac{D_\rho}{2}N^2\right)^l \tag{3.21}$$

$$\leqslant M_u^\rho \frac{2^{k+1}(k+1)\mathcal{L}(\mathcal{E}_\rho)}{\pi C_1(\rho,k)D_\rho^{2k+3}} \frac{\tilde{n}^{\frac{1}{2}}}{\rho^{\tilde{n}}} \left(1+\frac{D_\rho}{2}N^2\right)^k. \tag{3.22}$$

On the other hand, if $u_N(x) = u_{NB}(x)$, then $\omega_{N+1}(x) = (A_{\tilde{n}}^{k+1,k+1})^{-1}\mathcal{J}_{N+1}^{-(k+1),-(k+1)}(x)$. Similarly, we have:

$$D^l\omega_{N+1}(x) = (-2)^l \frac{\Gamma(N-2k+l)}{\Gamma(N-2k)} \mathcal{J}_{N+1-l}^{l-k-1,l-k-1}(x),\ l=0,1,\ldots,k+1. \tag{3.23}$$

when N is large enough. By Stirling's formula, we achieve

$$\max_{-1\leqslant x\leqslant 1}|D^l\omega_{N+1}(x)| \leqslant \frac{\Gamma(N-2k+l)\Gamma(N-k+1+l)}{2^{N-2k-1}\Gamma(N-2k)\Gamma(\frac{N-2k+1+l}{2})\Gamma(\frac{N+3+l}{2})} \tag{3.24}$$

$$\leqslant \frac{2^{k+2}}{\sqrt{\pi}}(\frac{2}{e})^l N^{l-\frac{1}{2}},\ l=0,\ldots,k. \tag{3.25}$$

Taking $l = k+1$ yields

$$\max_{-1\leqslant x\leqslant 1}|D^{k+1}\omega_{N+1}(x)| = 2^{k+1}\frac{\Gamma(N-k+1)}{\Gamma(N-2k)} \max_{-1\leqslant x\leqslant 1}|P_{N-k}^{0,0}(x)|$$
$$\leqslant 2^{k+1}N^{k+1}. \tag{3.26}$$

Again, $\forall \rho > 1, k \in \mathbb{N}$, $\exists C_2(\rho,k) > 0$, such that

$$\min_{z\in\mathcal{E}_\rho}|P_{\tilde{n}}^{k+1,k+1}(z)| \geqslant C_2(\rho,k)\tilde{n}^{-\frac{1}{2}}\rho^{\tilde{n}},$$

and for $\forall z \in \mathcal{E}_\rho$, we have

$$|(1+z)(1-z)| = \frac{1}{4}|(\rho e^{i\theta} - \rho^{-1}e^{-i\theta})^2| = \frac{1}{4}|(\rho-\rho^{-1})\cos\theta + i(\rho+\rho^{-1})\sin\theta|^2$$
$$= \frac{1}{4}[(\rho^2+\rho^{-2}-2)\cos^2\theta + (\rho^2+\rho^{-2}+2)\sin^2\theta]$$
$$= \frac{1}{4}(\rho-\rho^{-1})^2 + \sin^2\theta \geqslant \frac{1}{4}(\rho-\rho^{-1})^2.$$

Therefore

$$\min_{z\in\mathcal{E}_\rho}|\mathcal{J}_{N+1}^{-(k+1),-(k+1)}(z)| \geqslant \min_{z\in\mathcal{E}_\rho}|(1+z)(1-z)|^{k+1} \cdot \min_{z\in\mathcal{E}_\rho}|P_{\tilde{n}}^{k+1,k+1}(z)|$$
$$\geqslant \frac{(\rho-\rho^{-1})^{2k+2}}{4^{k+1}} C_2(\rho,k)\tilde{n}^{-\frac{1}{2}}\rho^{\tilde{n}}. \tag{3.27}$$

Similar to previous case, by inputing (3.25), (3.26) and (3.27) into (3.14), the proof is complete. □

Remark 3.3. Let $f(N;k,l)$ be defined by the right hand side in (3.24), *i.e.*

$$f(N;k,l) := \frac{\Gamma(N-2k+l)\Gamma(N-k+1+l)}{2^{N-2k-1}\Gamma(N-2k)\Gamma(\frac{N-2k+1+l}{2})\Gamma(\frac{N+3+l}{2})}. \tag{3.28}$$

In Figure 1, it shows that $f(N;k,l) = O(N^{l-\frac{1}{2}})$ when N is large enough. However, when N is small, especially $N \leqslant 30$, it is more likely that

$$f(N;k,l) \lesssim O(N^l).$$

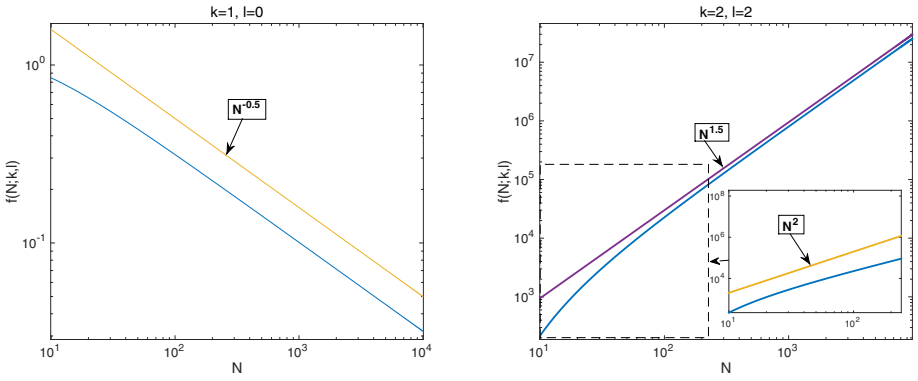

FIGURE 1. The graphs of $f(N;k,l)$ for $N \in [10, 10^4]$, where $k = 1$, $l = 0$ (*left panel*), $k = 2$, $l = 2$ (*right panel*).

Therefore, even though (3.11) and (3.12) in Theorem 3.2 show that the gain of convergence rate at superconvergence points is $O(N^{-\frac{3}{2}})$ when N is large enough. While $N \leqslant 30$, it seems the gain of convergence rate behaves like $O(N^{-1})$.

Remark 3.4. Similar to Chebyshev and Legendre interpolation, the three kinds of Hermite interpolations are exponentially convergent as well. Strictly speaking, they are exponentially convergent with respect to $\tilde{n}$, the number of interpolation points except for $x = \pm 1$, instead of N, the degree of interpolants. Therefore, it will significantly improve the accuracy to increase the number of inside interpolation points. On the other hand, for any fixed k, because of the exponential convergence rate, u_N converges to u very fast. So admissible results can be usually obtained when N is small.

Since all of the three kinds of superconvergence points are zero points of Jacobi polynomials, they can be efficiently calculated.

4. HERMITE INTERPOLATION FOR RIEMANN–LIOUVILLE DERIVATIVES WITH ARBITRARY POSITIVE ORDER

4.1. Theoretical statements

As mentioned in introduction, the Hermite interpolations are mainly designed to resolve the singularities of the fractional differential operators. Let $k < \alpha < k + 1$, where k is a nonnegative integer. For the left Riemann–Liouville fractional operator ${}_{-1}D_x^{\alpha}$ which is defined in (2.1), one can obviously observe that

$$(u - u_{NL})^{(l)}(-1) = 0, \ l = 0, 1, \ldots, k, \tag{4.1}$$

and ${}_{-1}D_x^{\alpha}(u(x) - u_{NL}(x))$ is bounded on $[-1, 1]$. As for the right Riemann–Liouville operator ${}_xD_1^{\alpha}$ defined in (2.2), similarly, we have

$$(u - u_{NR})^{(l)}(1) = 0, \ l = 0, 1, \ldots, k, \tag{4.2}$$

and ${}_xD_1^{\alpha}(u(x) - u_{NR}(x))$ is bounded on $[-1, 1]$ as well.

Remark 4.1. If interpolating in these ways, it is equivalent to take Riemann–Liouville derivative and Caputo derivative, so the following results also work for the Caputo fractional derivative.

Theorem 4.2. *Let $k < \alpha < k+1$, where k is a nonnegative integer. Let u_{NL} and u_{NR} be the interpolants defined in (3.1) and (3.2), respectively. Then*

$$\|{}_{-1}D_x^{\alpha}(u-u_{NL})\|_{L^{\infty}[-1,1]} \leqslant \frac{2^{k+1-\alpha}}{\Gamma(k+2-\alpha)}\|(u-u_{NL})^{(k+1)}\|_{L^{\infty}[-1,1]}; \tag{4.3}$$

$$\|{}_{x}D_1^{\alpha}(u-u_{NR})\|_{L^{\infty}[-1,1]} \leqslant \frac{2^{k+1-\alpha}}{\Gamma(k+2-\alpha)}\|(u-u_{NR})^{(k+1)}\|_{L^{\infty}[-1,1]}. \tag{4.4}$$

Proof. Without loss of generality, we only consider the poof of left Riemann–Liouville derivatives. According to (2.1), (4.1) and Hölder's inequality yields

$$\begin{aligned}
&|{}_{-1}D_x^{\alpha}(u(x)-u_{NL}(x))| \\
&\quad= \frac{1}{\Gamma(k+1-\alpha)}\Big|\int_{-1}^{x}\frac{(u-u_{NL})^{(k+1)}(t)}{(x-t)^{\alpha-k}}\mathrm{d}t\Big| \\
&\quad\leqslant \frac{\|(u-u_{NL})^{(k+1)}\|_{L^{\infty}}}{\Gamma(k+1-\alpha)}\int_{-1}^{x}(x-t)^{k-\alpha}\mathrm{d}t \\
&\quad= \frac{(1+x)^{k+1-\alpha}}{\Gamma(k+2-\alpha)}\|(u-u_{NL})^{(k+1)}\|_{L^{\infty}[-1,1]}, \forall x\in[-1,1].
\end{aligned} \tag{4.5}$$

Therefore,

$$\|{}_{-1}D_x^{\alpha}(u-u_{NL})\|_{L^{\infty}[-1,1]} \leqslant \frac{2^{k+1-\alpha}}{\Gamma(k+2-\alpha)}\|(u-u_{NL})^{(k+1)}\|_{L^{\infty}[-1,1]},$$

and in fact, $\forall\alpha\in(k,k+1)$, we always have:

$$\frac{2^{k+1-\alpha}}{\Gamma(k+2-\alpha)} \leqslant 2.$$

□

Remark 4.3. Even though Theorem 4.2 establishes the boundedness in the sense of L^{∞}-norm, it is not a sharp estimate as demonstrated by the following numerical example. We wonder if there exists $r>0$, s.t.

$$\|{}_{-1}D_x^{\alpha}(u-u_{NL})\|_{L^{\infty}[-1,1]} \lesssim N^{-r}\|(u-u_{NL})^{(k+1)}\|_{L^{\infty}[-1,1]}.$$

To further quantify it, we define the ratio as

$$r_1(N) = \frac{\|(u-u_{NL})^{(k+1)}\|_{L^{\infty}[-1,1]}}{\|{}_{-1}D_x^{\alpha}(u-u_{NL})\|_{L^{\infty}[-1,1]}}. \tag{4.6}$$

In this numerical experiment, we consider $f(x)=\frac{(1+x)^2}{1+4x^2}$, and take $\alpha\in(1,2)$. For any fixed α, we can evaluate the ratio for different N, and then estimate the value of r numerically. As what one can see in Table 1, $r=2(k+1-\alpha)$. Further theoretical investigation is required. The same discussion also applies to Theorem 5.1.

Parallel to the conclusion in [35], we have the following theorem.

Theorem 4.4. *Let $\alpha\in(k,k+1)$, let u_{NL} and u_{NR} be the interpolants defined in (3.1) and (3.2), respectively. The αth left Riemann–Liouville fractional derivative superconverges at $\{{}_L\xi_i^{\alpha}\}$ satisfying*

$${}_{-1}I_x^{k+1-\alpha}P_{N-k}^{k+1,0}({}_L\xi_i^{\alpha}) = 0,\ i=1,\dots,N-k. \tag{4.7}$$

Similarly, the αth right Riemann–Liouville fractional derivative superconverges at $\{{}_R\xi_i^{\alpha}\}$ satisfying

$${}_{x}I_1^{k+1-\alpha}P_{N-k}^{0,k+1}({}_R\xi_i^{\alpha}) = 0,\ i=1,\dots,N-k. \tag{4.8}$$

TABLE 1. The ratios of (4.6) for different αth-derivatives.

Derivative order (α)	$k+1-\alpha$	Order (r)
1.1	0.9	1.8089
1.3	0.7	1.4095
1.5	0.5	1.0104
1.6	0.4	0.8103
1.7	0.3	0.6086
1.9	0.1	0.2036

Proof. Again, we only give the proof of (4.7). The proof starts with (2.25). Similar to (3.13) for $\forall x \in [-1,1]$, we have

$$\begin{aligned} &{}_{-1}D_x^{\alpha}(u(x)-u_N(x)) \\ &\quad= \frac{1}{2\pi i}\oint_{\mathcal{E}_\rho} {}_{-1}D_x^{\alpha}\Big(\frac{\omega_{N+1}(x)}{z-x}\Big)\frac{u(z)}{\omega_{N+1}(z)}\mathrm{d}z \\ &\quad= \frac{1}{2\pi i}\oint_{\mathcal{E}_\rho} \sum_{m=0}^{\infty}\frac{\Gamma(\alpha+1)}{\Gamma(\alpha-m+1)}\frac{{}_{-1}D_x^{\alpha-m}\mathcal{J}_{N+1}^{0,-(k+1)}(x)}{(z-x)^{(m+1)}}\frac{u(z)}{\mathcal{J}_{N+1}^{0,-(k+1)}(z)}\mathrm{d}z. \end{aligned} \tag{4.9}$$

According to the analysis in [35], the decay of the error is dominated by the leading term:

$$\oint_{\mathcal{E}_\rho}\frac{{}_{-1}D_x^{\alpha}\mathcal{J}_{N+1}^{0,-(k+1)}(x)}{(z-x)}\frac{u(z)}{\mathcal{J}_{N+1}^{0,-(k+1)}(z)}\mathrm{d}z. \tag{4.10}$$

When we take $x = {}_L\xi_i^{\alpha}$, the roots of ${}_{-1}D_x^{\alpha}\mathcal{J}_{N+1}^{0,-(k+1)}(x)$, the leading term vanishes, and the remaining terms have higher-order convergence rates. While by Lemma 2.12, it can be simplified:

$$\begin{aligned} {}_{-1}D_x^{\alpha}\mathcal{J}_{N+1}^{0,-(k+1)}(x) &= D^{k+1}\,{}_{-1}I_x^{k+1-\alpha}\mathcal{J}_{N+1}^{0,-(k+1)}(x) \\ &= {}_{-1}I_x^{k+1-\alpha}D^{k+1}\mathcal{J}_{N+1}^{0,-(k+1)}(x) = \frac{\Gamma(N+2)}{\Gamma(N+1-k)}\,{}_xI_1^{k+1-\alpha}P_{N-k}^{k+1,0}(x). \end{aligned}$$

Therefore, we may identify the superconvergence points $\{{}_L\xi_i^{\alpha}\}_{i=1}^{N-k}$ as the roots of ${}_xI_1^{k+1-\alpha}P_{N-k}^{k+1,0}(x)$, which can be efficiently calculated by Theorem 4.5. □

4.2. Calculating the superconvergence points

The recurrence formulas of calculating ${}_{-1}I_x^{\gamma}P_n^{a,b}(x)$ and ${}_xI_1^{\gamma}P_n^{a,b}(x)$ are provided in (20) and (23), respectively in [30]. Therefore, we can calculate the zero points of ${}_{-1}I_x^{k+1-\alpha}P_{N-k}^{k+1,0}(x)$ and ${}_xI_1^{k+1-\alpha}P_{N-k}^{0,k+1}(x)$ by eigenvalue method.

Theorem 4.5. *The zeros $\{{}_L\xi_i\}_{i=1}^n$ of the function ${}_{-1}I_x^{\gamma}P_n^{a,b}(x)$ are eigenvalues of the following matrix $S_L \in \mathcal{M}_{n\times n}(\mathbb{R})$:*

$$\begin{pmatrix} S_{L11} & S_{L12} & & \cdots & & 0 \\ S_{L21} & S_{L22} & S_{L23} & & & \\ S_{L31} & S_{L32} & S_{L33} & S_{L34} & & \vdots \\ S_{L41} & 0 & S_{L43} & S_{L44} & \ddots & \\ \vdots & \vdots & 0 & \ddots & \ddots & S_{Ln-1,n} \\ S_{Ln1} & 0 & \cdots & 0 & S_{Ln,n-1} & S_{Lnn} \end{pmatrix}, \tag{4.11}$$

where

$$S_{L11} = \frac{b-a+2\gamma+2b\gamma}{a+b+2}; \quad S_{Lkk} = \frac{A_k^2}{A_k^1}, k = 2, \ldots, n;$$
$$S_{L12} = \frac{2(1+\gamma)}{a+b+2}; \quad S_{Lk,k+1} = \frac{1}{A_k^1}, k = 2, \ldots, n-1;$$
$$S_{L21} = \frac{A_2^3 - A_2^{L4}}{A_2^1}; \quad S_{Lk+1,k} = \frac{A_{k+1}^3}{A_{k+1}^1}, k = 2, \ldots, n-1;$$
$$S_{Lk,1} = -\frac{A_k^{L4}}{A_k^1}, k = 3, \ldots, n.$$

The zeros $\{{}_R\xi_i\}_{i=1}^n$ *of the function* ${}_xI_1^\gamma P_n^{a,b}(x)$ *are eigenvalues of the matrix* $S_R \in \mathcal{M}_{n\times n}(\mathbb{R})$*, which is of the same form as* S_L*, where*

$$S_{R11} = \frac{b-a-2\gamma-2a\gamma}{a+b+2}; \quad S_{Rkk} = \frac{A_k^2}{A_k^1}, k = 2, \ldots, n;$$
$$S_{R12} = \frac{2(1+\gamma)}{a+b+2}; \quad S_{Rk,k+1} = \frac{1}{A_k^1}, k = 2, \ldots, n-1;$$
$$S_{R21} = \frac{A_2^3 - A_2^{R4}}{A_2^1}; \quad S_{Rk+1,k} = \frac{A_{k+1}^3}{A_{k+1}^1}, k = 2, \ldots, n-1;$$
$$S_{Rk,1} = -\frac{A_k^{R4}}{A_k^1}, k = 3, \ldots, n,$$

when $2 \leqslant k \leqslant n$*,*

$$A_k^1 = \frac{\tilde{a}_k}{1+\gamma\tilde{a}_k\bar{c}_k}, \ A_k^2 = \frac{\tilde{b}_k+\gamma\tilde{a}_k\bar{b}_k}{1+\gamma\tilde{a}_k\bar{c}_k}, \ A_k^3 = \frac{\tilde{c}_k+\gamma\tilde{a}_k\bar{a}_k}{1+\gamma\tilde{a}_k\bar{c}_k},$$
$$A_k^{L4} = \frac{\gamma\tilde{a}_k(\bar{a}_k d_k^{L1} + \bar{b}_k d_k^{L2} + \bar{c}_k d_k^{L3})}{(1+\gamma\tilde{a}_k\bar{c}_k)}, \ A_k^{R4} = \frac{\gamma\tilde{a}_k(\bar{a}_k d_k^{R1} + \bar{b}_k d_k^{R2} + \bar{c}_k d_k^{R3})}{(1+\gamma\tilde{a}_k\bar{c}_k)},$$

where

$$\tilde{a}_k = \frac{(2k-1+a+b)(2k+a+b)}{2k(k+a+b)}, \quad \tilde{b}_k = \frac{(b^2-a^2)(2k-1+a+b)}{2k(k+a+b)(2k-2+a+b)},$$
$$\tilde{c}_k = \frac{(k-1+a)(k-1+b)(2k+a+b)}{k(k+a+b)(2k-2+a+b)},$$
$$\bar{a}_k = \frac{-2(k-1+a)(k-1+b)}{(k-1+a+b)(2k-2+a+b)(2k-1+a+b)},$$
$$\bar{b}_k = \frac{2(a-b)}{(2k-2+a+b)(2k+a+b)}, \quad \bar{c}_k = \frac{2(k+a+b)}{(2k-1+a+b)(2k+a+b)},$$
$$d_k^{L1} = (-1)^k\binom{k-2+b}{k-2}, \quad d_k^{L2} = (-1)^{k-1}\binom{k-1+b}{k-1}, \quad d_k^{L3} = (-1)^k\binom{k+b}{k},$$
$$d_k^{R1} = \binom{k-2+a}{k-2}, \quad d_k^{R2} = \binom{k-1+a}{k-1}, \quad d_k^{R3} = \binom{k+a}{k}.$$

Proof. The recurrence formula for left integral of Jacobi polynomial, ${}_{-1}I_x^{\gamma}P_n^{a,b}(x)$ is given by, seeing [30] (20):

$$\begin{cases} {}_{-1}I_x^{\gamma}P_0^{a,b}(x) &= \frac{(1+x)^{\gamma}}{\Gamma(\gamma+1)}, \\ {}_{-1}I_x^{\gamma}P_1^{a,b}(x) &= \frac{a+b+2}{2}(x[{}_{-1}I_x^{\gamma}P_0^{a,b}(x)] - \frac{\gamma(1+x)^{\gamma+1}}{\Gamma(\gamma+2)}) \\ &\quad + \frac{a-b}{2}[{}_{-1}I_x^{\gamma}P_0^{a,b}(x)], \\ {}_{-1}I_x^{\gamma}P_{k+1}^{a,b}(x) &= (A_{k+1}^1 x - A_{k+1}^2)[{}_{-1}I_x^{\gamma}P_k^{a,b}(x)] - A_{k+1}^3[{}_{-1}I_x^{\gamma}P_{k-1}^{a,b}(x)] \\ &\quad + A_{k+1}^{L4}[{}_{-1}I_x^{\gamma}P_0^{a,b}(x)], \quad k = 1, \ldots, n-1, \end{cases} \tag{4.12}$$

and the formula for right integral, ${}_xI_1^{\gamma}P_n^{a,b}(x)$, is given by, seeing [30] (23):

$$\begin{cases} {}_xI_1^{\gamma}P_0^{a,b}(x) &= \frac{(1-x)^{\gamma}}{\Gamma(\gamma+1)}, \\ {}_xI_1^{\gamma}P_1^{a,b}(x) &= \frac{a+b+2}{2}(x[{}_xI_1^{\gamma}P_0^{a,b}(x)] + \frac{\gamma(1-x)^{\gamma+1}}{\Gamma(\gamma+2)}) \\ &\quad + \frac{a-b}{2}[{}_xI_1^{\gamma}P_0^{a,b}(x)], \\ {}_{-1}I_x^{\gamma}P_{k+1}^{a,b}(x) &= (A_{k+1}^1 x - A_{k+1}^2)[{}_xI_1^{\gamma}P_k^{a,b}(x)] - A_{k+1}^3[{}_xI_1^{\gamma}P_{k-1}^{a,b}(x)] \\ &\quad + A_{k+1}^{R4}[{}_xI_1^{\gamma}P_0^{a,b}(x)], \quad k = 1, \ldots, n-1, \end{cases} \tag{4.13}$$

where $A_k^1, A_k^2, A_k^3, A_k^{L4}, A_k^{R4}$, $k = 1, 2, \ldots, n-1$, are given in the statement of the theorem. The rest of proof is parallel to the Theorem 3.4 in [21]. □

5. Hermite interpolation for Riesz derivatives with arbitrary positive order

Parallel to the previous section, there are similar conclusions for Riesz fractional derivatives.

Theorem 5.1. *Let $k < \alpha < k+1$, where k is a nonnegative integer. Let u_{NB} be the interpolant defined in (3.3), respectively. Then we have:*

$$\|{}^RD^{\alpha}(u - u_{NB})\|_{L^{\infty}[-1,1]} \leqslant \frac{2C_R}{\Gamma(k+2-\alpha)}\|(u - u_{NB})^{(k+1)}\|_{L^{\infty}[-1,1]}, \tag{5.1}$$

where $C_R = \max\{c1, c2\}$, both $c1, c2$ are defined in (2.5).

Proof. It is a direct corollary of (2.5), (4.5) and the fact that:

$$\max_{-1 \leqslant x \leqslant 1}\{(1+x)^{\gamma} + (1-x)^{\gamma}\} = 2, \ \forall \gamma \in (0,1).$$

□

Remark 5.2. Theorems 4.2 and 5.1 state that if the $(k+1)$-th derivative of $(u - u_N)$ converges, then the αth derivative of $(u - u_N)$ must converge with at least the same convergence rate.

The superconvergence points are located by the following theorem.

Theorem 5.3. *Let $\alpha \in (k, k+1)$, let u_{NB} be the interpolant defined in (3.3). The αth Riesz fractional derivative superconverges at $\{{}_B\xi_i^{\alpha}\}$, which satisfies*

$${}^RD^{\alpha}\mathcal{J}_{N+1}^{-(k+1),-(k+1)}({}_B\xi_i^{\alpha}) = 0, \ i = 1, \ldots, N-1. \tag{5.2}$$

Proof. The framework of the proof is the same as Theorem 4.4. □

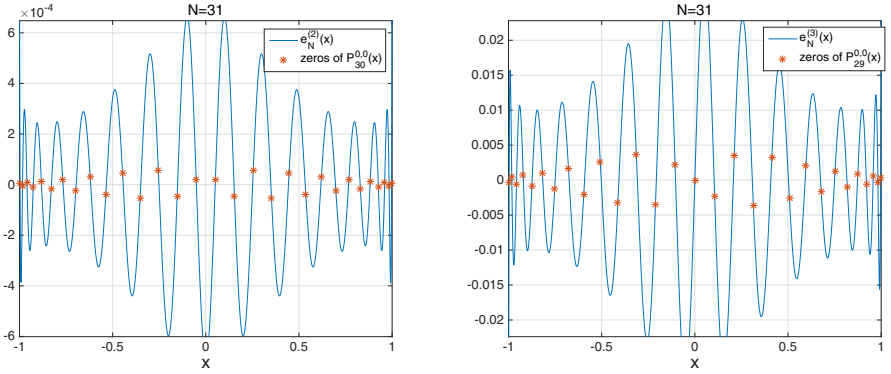

FIGURE 2. (Example 6.1) *Left panel*: the second derivative of error $e_N^{(2)}(x)$ with $N = 31$ and the zeros of $P_{30}^{0,0}(x)$. *Right panel*: the third derivative of error $e_N^{(3)}(x)$ with $N = 31$ and zeros of $P_{29}^{0,0}(x)$.

6. Numerical examples

We use Examples 6.1–6.3 to investigate the superconvergence points for integer-order derivatives, Riemann fractional derivatives, and Riesz fractional derivatives, respectively. After that, we apply the theoretical results to solve the integer-order/fractional boundary value problems to illustrate the effectiveness of the theoretical analysis and application of superconvergence points.

6.1. Superconvergence in derivatives of interpolations

For the convenience of notations, we define $e_N(x) := f(x) - f_N(x)$.

Example 6.1. Set $f(x) = \frac{1}{1+4x^2}$, which is an analytic function with two simple poles $z = \pm\frac{i}{2}$ in the complex plane. Take the degree of interpolation polynomial $N = 31$. Noting that $f(x)$ is even, we apply two-point Hermite interpolations to demonstrate the superconvergence points as shown in Theorem 3.2 with the following two cases.

Case 1. Assume that the errors satisfy $e_N(-1) = e_N(1) = e'_N(-1) = e'_N(1) = 0$. Left panel of Figure 2 shows that the second derivative of $e'_N(x)$, and the superconvergence points predicted as the zeros of $P_{30}^{0,0}(x)$ based on Theorem 3.2.

Case 2. Assume that the errors satisfy $e_N(-1) = e_N(1) = e'_N(-1) = e''_N(1) = e''_N(1) = e''_N(-1) = 0$. Right panel of Figure 2 shows the third derivative of $e'''_N(x)$, and the superconvergence points predicted as the zeros of $P_{29}^{0,0}(x)$ based on Theorem 3.2.

Example 6.2. This example is used to observe the superconvergence phenomenon for Riemann–Liouville derivatives by taking $f(x) = \frac{1}{10}(1+x)^{6.15}$, $N = 18$, and $\alpha = 1.23, 1.78, 2.23, 2.78$, respectively. Two cases are also considered.

Case 1 ($1 < \alpha < 2$). In this situation, we set $e_N(-1) = e'_N(-1) = 0$ by adopting the interpolation (3.1). Left panel of Figure 3 shows the errors ${}_{-1}D_x^{\alpha} e_N(x)$ with $\alpha = 1.23, 1.78$, and the superconvergence points predicted as zeros of ${}_{-1}I_x^{2-\alpha} P_{17}^{2,0}(x)$ based on Theorem 4.4.

Case 2 ($2 < \alpha < 3$). In this situation, we set $e_N(-1) = e'_N(-1) = e''_N(-1) = 0$ by adopting the interpolation (3.1) again. Right panel of Figure 3 shows the errors ${}_{-1}D_x^{\alpha} e_N(x)$ with $\alpha = 2.23, 2.78$, and the superconvergence points predicted as zeros of ${}_{-1}I_x^{3-\alpha} P_{16}^{3,0}(x)$ based on Theorem 4.4.

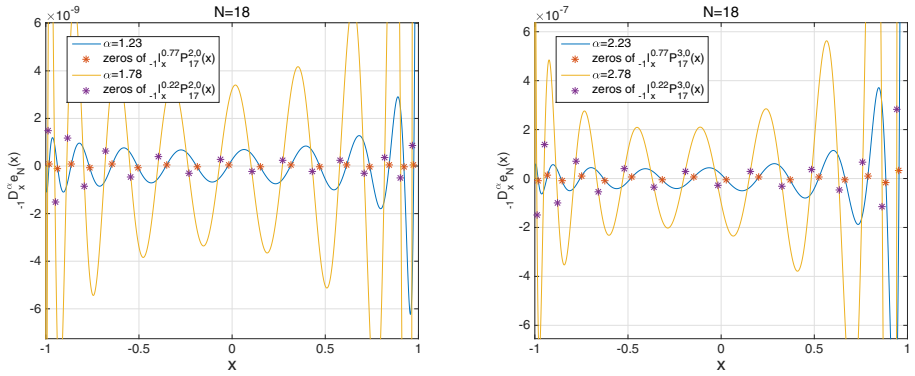

FIGURE 3. (Example 6.2) *Left panel*: Riemann–Liouville derivative errors ${}_{-1}D_x^{\alpha}e_N(x)$, and the superconvergence points predicted as zeros of ${}_{-1}I_x^{2-\alpha}P_{17}^{2,0}(x)$ with $N = 18$ and $\alpha = 1.23, 1.78$. *Right panel*: the errors ${}_{-1}D_x^{\alpha}e_N(x)$, and the superconvergence points predicted as zeros of ${}_{-1}I_x^{3-\alpha}P_{16}^{3,0}(x)$ with $N = 18$ and $\alpha = 2.23, 2.78$.

TABLE 2. Superconvergence ratios of (6.1) for different αth-derivatives.

Derivative order (α)	Gain of rate (β)	Derivative order (α)	Gain of rate (β)
1.13	1.43	2.13	1.65
1.33	1.51	2.33	1.66
1.53	1.47	2.53	1.68
1.73	1.52	2.73	1.71
1.93	1.52	2.93	1.73

To further quantify the superconvergence rate, we define the superconvergence ratio as

$$r_2(N) = \frac{\max_{-1\leqslant x\leqslant 1} |{}^R D^{\alpha}(u - u_N)(x)|}{\max_{0\leqslant i\leqslant n} |{}^R D^{\alpha}(u - u_N)(\xi_i^{\alpha})|}. \tag{6.1}$$

According to (3.6), $r_2(N)$ is exactly N^{β}. For any fixed α, we can evaluate the ratio for different N values, and then estimate the gain of rate β numerically. As what one can see in Table 2, the convergence rates at the superconvergence points are at least $O(N^{-1})$, for different α, higher than the global rate, and the gain of convergence rate increases while the derivative order is increasing.

Example 6.3. This example is used to investigate the superconvergence for Riesz fractional derivatives by taking $f(x) = (1 + x)^9(1 - x)^9$, and $\alpha = 1.62, 2.44$. The function is interpolated at zeros of $\mathcal{J}_{18}^{-2,-2}(x)$ for $\alpha = 1.62$, and at zeros of $\mathcal{J}_{18}^{-3,-3}(x)$ for $\alpha = 2.44$, respectively. Similar to previous examples, the errors of ${}_{-1}D_x^{\alpha}e_N(x)$ are shown, and the superconvergence points are highlighted in the Figure 4 respectively.

In all simulations above, we can observe that the error at highlighted points is much less than the global error.

Example 6.4. This example is used to study the performance of superconvergence points for nonsmooth underlying functions by taking $f(x) = \frac{(1+x)^{\alpha}}{1+x^2}$, and $\alpha = 1.6$, where $\frac{1}{1+x^2}$ is an analytic function, and $f''(x)$ is not bounded in the L^{∞} sense. In the simulation, we set $e_N(-1) = e_N'(-1) = 0$ by adopting the interpolation (3.1). Left panel of Figure 5 shows the error ${}_{-1}D_x^{\alpha}e_N(x)$ with $N = 8, 12, 16$, respectively, and the right panel shows the error of $N = 16$ and the superconvergence points predicted as zeros of ${}_{-1}I_x^{2-\alpha}P_{15}^{2,0}(x)$ based on Theorem 4.4.

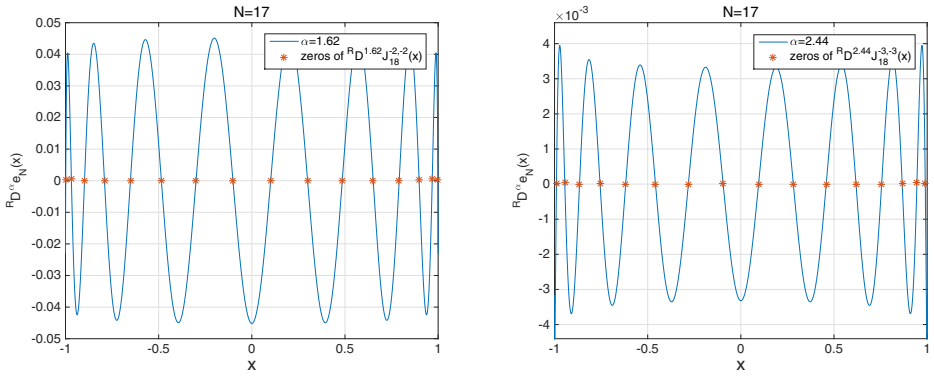

FIGURE 4. (Example 6.3) *Left panel*: Riesz fractional derivative errors ${}^{R}D^{\alpha}e_N(x)$ with $\alpha = 1.62$. *Right panel*: the errors ${}^{R}D^{\alpha}e_N(x)$ with $\alpha = 2.44$.

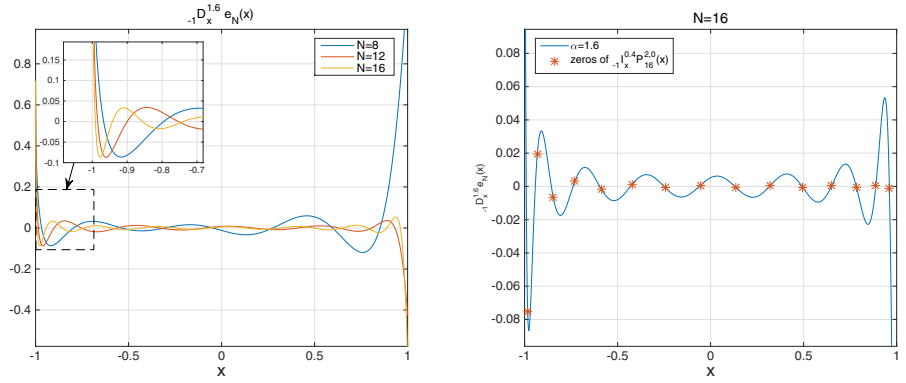

FIGURE 5. (Example 6.4) *Left panel*: Riemann–Liouville derivative errors ${}_{-1}D_x^{\alpha}e_N(x)$ with $N = 8, 12, 16$ and $\alpha = 1.6$. *Right panel*: the errors ${}_{-1}D_x^{\alpha}e_N(x)$, and the superconvergence points predicted as zeros of ${}_{-1}I_x^{2-\alpha}P_{15}^{2,0}(x)$ with $N = 16$ and $\alpha = 1.6$.

In the left panel, we observe that the error ${}_{-1}D_x^{\alpha}e_N(x)$ does not converge to 0 with N increasing, especially when x is near the boundary. The reason is that the interpolant does not fit the singularity at the end-points: $f(x) = O((1+x)^{1.6})$ while $f_N(x) = O((1+x)^2)$ near $x = -1$. In the right panel, when x is near -1, the performance of those superconvergence points is not good. Nevertheless, in the interior, where $f(x)$ is smooth, the error at highlighted points is still much less than the global error. We see that the Hermite interpolation (polynomial interpolation) is not a good choice if the underlying function contains singular term, and the low regularity affects the performance of superconvergence points indeed. To approximate nonsmooth functions, non-polynomial basis functions (such as the GJF fractional interpolation introduced in [7]) that reflect the singular behaviors are preferred.

6.2. Applications

We now apply superconvergence points above to solve integer-order/fractional boundary value problems, and investigate the effectiveness of our theoretical analysis.

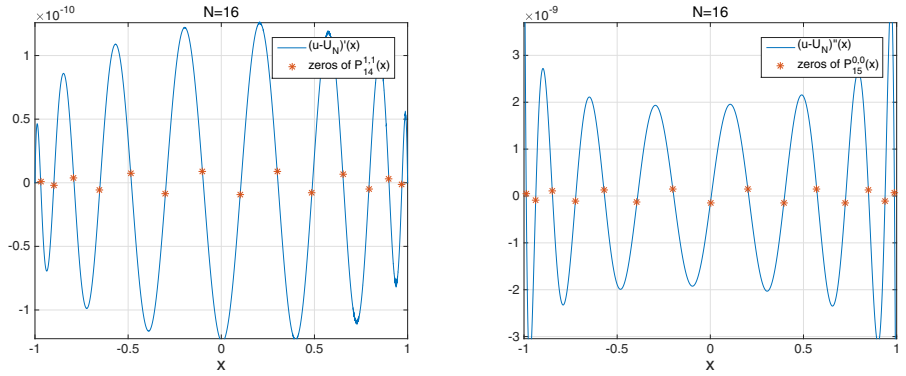

FIGURE 6. *Left panel*: the first derivative error: $e_N'(x)$, with $N = 16$; the zeros of $P_{14}^{1,1}(x)$ are asterisked. *Right panel*: the second derivative error: $e_N''(x)$, with $N = 16$; the Gauss points are asterisked.

Example 6.5. Consider the following fourth-order boundary value problem:

$$\begin{cases} u^{(4)}(x) + u(x) = f(x), \ x \in (-1, 1), \\ u(-1) = u'(-1) = u(1) = u'(1) = 0. \end{cases} \tag{6.2}$$

To illustrate the quantitative pictures to the behavior of numerical solutions, we take the exact solution in the form of $u(x) = a_0 + 30e^x + a_2 e^{1.5x} + a_3 e^{2x} + a_4 e^{2.5x}$, where the coefficients a_0, a_2, a_3, a_4 and $f(x)$ can be calculated by using boundary conditions and the exact solution itself. Numerical solutions are obtained by the spectral-Galerkin method, see the detailed numerical scheme provided in ([21], Chap. 6). Left panel of Figure 6 shows the error of the first derivative $(u - U_N)'(x)$, and the first derivative superconverge points at the interior zeros of $\mathcal{J}_N^{-1,-1}(x)$ based on the analysis of Theorem 3.2. Similarly, right panel of Figure 6 shows the error of $(u - U_N)''(x)$, and the second derivative superconvergens at Guass points.

Example 6.6. Consider the fractional boundary value problem:

$$\begin{cases} {}_{-1}D_x^{\alpha} u(x) = f(x), \ x \in (-1, 1), \quad 1 < \alpha < 2, \\ u(-1) = u'(-1) = 0. \end{cases} \tag{6.3}$$

Again, to illustrate the quantitative pictures to the behavior of numerical solutions, we set the exact solution $u(x) = \frac{1}{10}(1 + x)^{6.15}$, and $f(x)$ can be calculated correspondingly. The problem (6.3) is solved by spectral-collocation methods. According to the original collocation method, let $\{x_i\}_{i=1}^{10}$ be the interior zeros of $\mathcal{J}_{12}^{0,-2}(x)$. The numerical solution can be written in the form of

$$U_N^o(x) = \sum_{j=1}^{N-1} U_j^o \hat{\ell}_j(x) := \sum_{j=1}^{N-1} U_j^o \cdot \ell_j(x) \frac{(1 + x)^2}{(1 + x_j)^2}, \tag{6.4}$$

where $\ell_j \in \mathbb{P}_N[-1, 1]$ is the Lagrange basis function satisfying

$$\ell_j(x_i) = \delta_{ij}, \ i, j = 1, \ldots, N - 1.$$

Hence, the numerical solution is to find $\mathbf{U}^o = (U_1^o, U_2^o, \ldots, U_{N-1}^o)^T \in \mathbb{R}^{N-1}$ such that

$$({}_{-1}D_x^{\alpha} U_N^o)(x_i) = f(x_i), \quad i = 1, \ldots, N - 1. \tag{6.5}$$

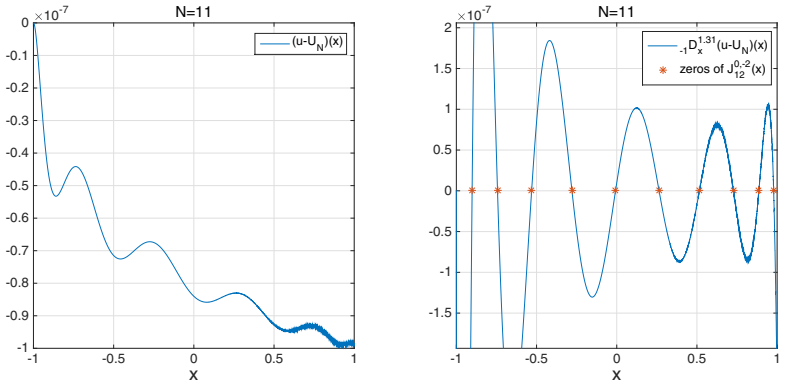

FIGURE 7. *Right panel*: fractional derivative errors: ${}_{-1}D_x^{1.31}e_N(x)$, with $N = 11$, evaluating points $\{x_i\}_{i=1}^{10}$ (asterisked). *Left panel*: the error $e_N(x)$, the curve doesn't oscillate around 0.

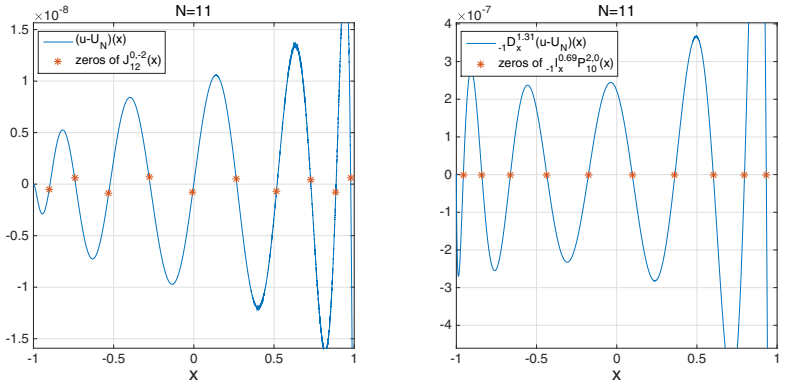

FIGURE 8. *Right panel*: fractional derivative errors: ${}_{-1}D_x^{1.31}e_N(x)$, with $N = 11$, evaluating points $\{\xi_i\}_{i=1}^{10}$ (asterisked). *Left panel*: the error $e_N(x)$, the curve oscillates around 0, and the error at the asterisked points (interpolation points) is much less than the global error.

TABLE 3. The comparison of maximal errors of the two collocation methods

N	6	7	8	9	10	11
E_o	6.45E-04	4.52E-05	6.46E-06	1.29E-06	3.32E-07	9.84E-08
E_n	3.42E-06	3.52E-07	5.54E-08	1.15E-08	2.90E-09	8.55E-10

In the simulation, we set $\alpha = 1.31$, $N = 11$. Left panel of Figure 7 shows the error $(u - U_N^o)(x)$, and right panel of Figure 7 shows the fractional derivative of error ${}_{-1}D_x^{\alpha}(u - U_N^o)(x)$ and the corresponding interpolation points. From Figure 7, one can see that that ${}_{-1}D_x^{\alpha}(u - U_N^o)(x)$ vanishes at $\{x_i\}_{i=1}^{10}$, but the error $(u - U_N^o)(x)$ doesn't have superconvergence phenomenon, since it doesn't oscillate around 0.

Based on the theoretical analysis in this paper, we may modify the numerical scheme (6.5) as: find $\mathbf{U}^n = (U_1^n, U_2^n, \ldots, U_{N-1}^n)^T \in \mathbb{R}^{N-1}$ such that

$$({}_{-1}D_x^{\alpha}U_N^n)(\xi_i) = f(\xi_i), \quad i = 1, \ldots, N-1, \tag{6.6}$$

where $\{\xi_i\}_{i=1}^{10}$, the zeros of ${}_{-1}I_x^{2-\alpha}P_{10}^{2,0}(x)$, are the superconvergence points predicted in Theorem 4.4. As proved above, Theorem 4.5 guarantees that the number of the superconvergence points $\{\xi_i\}$ is as same as of interpolation points $\{x_i\}$, so that the linear system has unique solution.

As what shown in Figure 8, one can observe that ${}_{-1}D_x^{\alpha}(u-U_N^n)(x)$ vanishes at $\{\xi_i\}_{i=1}^{10}$. More importantly, $U_N^n(x)$ superconverges to $u(x)$ at the interpolation points $\{x_i\}_{i=1}^{10}$. This leads that numerical solution of our new scheme (6.6) is much more accurate than that of the traditional scheme (6.5). To illustrate the accuracy of numerical schemes, for any given degree of freedom N, we define the maximum norms of numerical solutions respectively for schemes (6.5) and (6.6) as

$$E_o = \max_{1\leqslant i\leqslant N-1}\{|u(x_i)-U_i^o|\}, \text{ and } E_n = \max_{1\leqslant i\leqslant N-1}\{|u(x_i)-U_i^n|\}.$$

The maximal error norms E_o and E_n are list Table 3. One can see that for each N, E_n is significantly smaller than E_o at least by 10^{-2}.

7. Conclusions

Generally, the three kinds of Hermite interpolations are comparable to Lagrange-type spectral interpolations. It is proved that for any fixed k, the integer-order derivatives of the error decay exponentially with respect to the degree of freedom. The superconvergence points of each Hermite interpolation are also identified. Moreover, the convergence rates at the superconvergence points of the one-point and two-point Hermite interpolations are proved to be $O(N^{-2})$ and $O(N^{-\frac{3}{2}})$ higher than the global rate, respectively.

The superconvergence points of the Riemann–Liouville derivative can be efficiently and accurately calculated by an eigenvalue method. Numerical simulations show that the gain of convergence rate is at least $O(N^{-1})$. It is a future work to validate the gain of convergence rate for fractional derivatives theoretically. Another interesting observation is that the number of interpolation points for the Riemann–Liouville derivatives is equal to the number of superconvergence points, which differs from the case of integer-order derivatives. Therefore, we can use the superconvergence points found in this paper to numerically solve FDEs. By modifying the collocation scheme based on the analysis in Theorem 4.4, the errors at interpolation points are much smaller than the global errors. This phenomenon is not observed in the numerical solution of the traditional collocation method. Thus, comparing this with the traditional collocation method, our new scheme produces more accurate numerical solutions.

As far as we know, this is the first attempt to study the superconvergence points for Riemann–Liouville and Riesz fractional derivatives by using Hermite interpolation. As shown in [4, 9, 10, 13, 15, 17, 29, 31, 32, 37], spectral methods have successfully been applied to solve FDEs. The results in this paper will be useful to numerically solve FDEs, especially when using spectral collocation methods. Hence, it will be interesting to develop new spectral collocation methods based on the superconvergence points for high-order FDEs, such as the super-diffusion models in [14, 25], or FDEs with Riesz, Caputo, or two-sided fractional derivatives in [6, 11, 18, 22, 24, 31, 36].

Acknowledgements. This work is supported in part by the National Natural Science Foundation of China under grants NSFC 11471031, NSFC 91430216, NSFC 11771035, and NSAF U1530401; the US National Science Foundation through grant DMS-1419040.

References

[1] R. Askey, Orthogonal Polynomials and Special Functions. IAM, Philadelphia (1975).

[2] S.N. Bernstein, Sur l'ordre de la meilleure approximation des foncions continues par des polynomes de degré donné, Mém. *Publ. Class Sci. Acad. Belgique* **4** (1912) 1–103.

[3] W. Bu, Y. Tang and J. Yang, Galerkin finite element method for two-dimensional Riesz space fractional diffusion equations. *J. Comput. Phys.* **276** (2014) 26–38.

[4] S. Chen, J. Shen and L.-L. Wang, Generalized Jacobi functions and their applications to fractional differential equations. *Math. Comput.* **85** (2016) 1603–1638.

[5] P.J. Davis, Interpolation and Approximation. Dover, New York, NY (1975).

[6] K. Deng and W. Deng, Finite difference/predictor-corrector approximations for the space and time fractional Fokker–Planck equation. *Appl. Math. Lett.* **25** (2012) 1815–1821.

[7] B. Deng, Z. Zhang and X. Zhao, Superconvergence points for the spectral interpolation of Riesz fractional derivatives. Preprint arXiv:1709.10223 (2017).

[8] B.-Y. Guo, J. Shen and L.-L. Wang, Generalized Jacobi polynomials/functions and their applications. *Appl. Numer. Math.* **59** (2009) 1011–1028.

[9] C. Huang, Y. Jiao, L.-L. Wang and Z. Zhang, Optimal fractional integration preconditioning and error analysis of fractional collocation method using nodal Generalized Jacobi functions. *SIAM J. Numer. Anal.* **54** (2016) 3357–3387.

[10] C. Huang, Z. Zhang and Q. Song, Spectral methods for substantial fractional differential equations. *J. Sci. Comput.* **74** (2018) 1554–1574.

[11] N. Kopteva and M. Stynes, An efficient collocation method for a Caputo two-point boundary value problem. *BIT Numer. Math.* **55** (2015) 1105–1123.

[12] S. Lei and H. Sun, A circulant preconditioner for fractional diffusion equations. *J. Comput. Phys.* **242** (2013) 715–725.

[13] X. Li and C.J. Xu, A space-time spectral method for the time fractional diffusion equation. *SIAM J. Numer. Anal.* **47** (2009) 2108–2131.

[14] C. Li, Z. Zhao and Y.Q. Chen, Numerical approximation of nonlinear fractional differential equations with subdiffusion and superdiffusion. *Comput. Math. Appl.* **62** (2011) 855–875.

[15] C.P. Li, F.H. Zeng and F. Liu, Spectral approximations to the fractional integral and derivative. *Frac. Calc. Appl. Anal.* **15** (2012) 383–406.

[16] Q. Lin and J. Lin, Finite element methods: accuracy and improvement. *Mathematics Monograph Series 1*. Science Press, Beijing (2006).

[17] Z. Mao, S. Chen and J. Shen, Efficient and accurate spectral method using generalized Jacobi functions for solving Riesz fractional differential equations. *Appl. Numer. Math.* **106** (2016) 165–181.

[18] Z. Mao and G. Karniadakis, A spectral method (of exponential convergence) for singular solutions of the diffusion equation with general two-sided fractional derivative. *SIAM J. Numer. Anal.* **56** (2018) 24–49.

[19] H. Pang and H. Sun, Multigrid method for fractional diffusion equations. *J. Comput. Phys.* **231** (2012) 693–703.

[20] J.P. Roop, Computational aspects of FEM approximation of fractional advection dispersion equations on bounded domains in $\mathbb{R}^2$. *J. Comput. Appl. Math.* **193** (2006) 243–268.

[21] J. Shen, T. Tang and L-L. Wang, Spectral Methods: algorithms, analysis and applications. In Vol. 41 of *Springer Series in Computational Mathematics*. Springer (2011).

[22] S. Shen, F. Liu, V. Anh, I. Terner and J. Chen, A novel numerical approximation for the space fractional advection-dispersion equation. *IMA J. Appl. Math.* **79** (2014) 421–444.

[23] J. Shen, C. Sheng and Z. Wang, Generalized Jacobi spectral-Galerkin method for nonlinear Volterra integral equations with weakly singular kernels. *J. Math. Study* **48** (2015) 315–329.

[24] M. Stynes and L. Gracia, A finite difference method for a two-point boundary value problem with a Caputo fractional derivative. *IMA J. Numer. Anal.* **35** (2015) 698–721.

[25] C. Tadjeran and M.M. Meerschaert, A second-order accurate numerical method for the two-dimensional fractional diffusion equation. *J. Comput. Phys.* **220** (2007) 813–823.

[26] L.B. Wahlbin, Superconvergence in Galerkin finite element methods. In Vol. 1605 of *Lecture Notes in Math.* Springer-Verlag, Berlin (1995).

[27] L.-L. Wang, X.D. Zhao and Z. Zhang, Superconvergence of Jacobi–Gauss-type spectral interpolation. *J. Sci. Comput.* **59** (2014) 667–687.

[28] Z. Xie, L. Wang and X. Zhao, On exponential convergence of Gegenbauer interpolation and spectral differentiation. *Math. Comput.* **82** (2012) 1017–1036.

[29] Q. Xu and J.S. Hesthaven, Stable multi-domain spectral penalty methods for fractional partial differential equations. *J. Comput. Phys.* **257** (2014) 241–258.

[30] F. Zeng and C. Li, Fractional differential matrices with applications. Preprint arXiv:1404.4429 (2014).

[31] F. Zeng, F. Liu, C.P. Li, K. Burrage, I. Turner and V. Anh, Crank–Nicolson ADI spectral method for the 2-D Riesz space fractional nonlinear reaction-diffusion equation. *SIAM J. Numer. Anal.* **52** (2014) 2599–2622.

[32] F. Zeng, Z. Zhang and G. Karniadakis, A generalized spectral collocation method with tunable accuracy for variable-order fractional differential equations. *SIAM J. Sci. Comput.* **37** (2015) A2710–A2732.

[33] Z. Zhang, Superconvergence of a Chebyshev spectral collocation method. *J. Sci. Comput.* **34** (2008) 237–246.

[34] Z. Zhang, Superconvergence points of polynomial spectral interpolation. *SIAM J. Numer. Anal.* **50** (2012) 2966–2985.

[35] X. Zhao and Z. Zhang, Superconvergence points of fractional spectral interpolation. *SIAM J. Sci. Comput.* **38** (2016) A598–A613.

[36] X. Zhao, Z. Sun and Z. Hao, A fourth-order compact ADI scheme for two-dimensional nonlinear space fractional Schrödinger equation. *SIAM J. Sci. Comput.* **36** (2014) 2865–2886.

[37] M. Zheng, F. Liu, I. Turner and V. Anh, A novel high order space-time spectral method for the time-fractional Fokker–Planck equation. *SIAM J. Sci. Comput.* **37** (2015) A701–A724.